

Density waves and jamming transition in cellular automaton models for traffic flow

L. Neubert^a, H.Y. Lee^b, M. Schreckenberg^a

^a FB 10, Theoretische Physik, Gerhard-Mercator-Universität Duisburg, 47048 Duisburg, Germany

^b Dept. of Physics and Centre for Theoretical Physics, Seoul National University, Seoul 151-742, South Korea

Abstract

We present results of numerical investigations of the Nagel-Schreckenberg model, a microscopic traffic flow model based on a cellular automaton. This model exhibits a jamming transition with increasing vehicular density from a free-flow phase to a congested phase. The transition manifests in the behavior of the auto-correlation function which permits the determination of the velocity of upstream moving density waves. The numerical examinations are extended on two modifications of the standard cellular automaton, the slow-to-start model and the T² model. We investigate the jam velocity depending on several parameters and the auto-correlation function itself, we figure out the close interrelations between our measurements and the fundamental diagram of traffic flow and give a brief comparison with real traffic data.

I. INTRODUCTION

Recently, the examination and modeling of vehicular traffic became an important subject of research – see [1–6] and references therein for a brief review. In the microscopic approach to the traffic flow problem, the cellular automaton introduced in [7] reproduces important entities of real traffic, like the flow-density relation or stop-and-go waves. Beside the realization of some basic requirements to such a model it can be efficiently used in computational investigations and applications [8–10]. This is due to the simplicity of its rules. The simulation of real traffic as we know it by our daily experiences can be performed using multi-lane rules and vehicle- or road-dependent parameters [10,11]. Fundamental analytical and numerical examinations enclose exact solutions for certain limits and mean-field approximations [12–14], the jamming transition [15,16] or the effects of perturbations and the occurrence of metastable states [17,18], exemplary.

We investigate the density waves and the separation of the considered systems in free-flow and dense regions by the auto-correlation function. It enables us to trace back the spatiotemporal evolution of jams which are stable when a critical global density ρ_c is exceeded. It will be shown that the jamming transition is observable for varying both the global density ρ and the global noise p_{dec} . The jam velocity can be derived directly from the auto-correlation function and it is associated with the fundamental diagram which renders

the global flow-density relation. A further subject of interest are modifications of the standard cellular automaton, but it will be proved that the explanations for the jam velocity are also applicable.

The present paper is arranged as follows: Section 2 is devoted to the explanation of the underlying model and two of its modifications. These modifications are characterized by a particular treatment of standing vehicles with regard to their headways. In section 3 we introduce our measurement methods. The auto-correlation function $C_{v_j}(r, \tau)$ is suitable to determine jam velocities and to estimate the critical density ρ_c as well as the critical noise p_c where stable density waves emerge. Furthermore, we will discuss the results of our numerical simulations with regard to the dependences on the global density and the maximum velocity, for instance. Concluding, we will give a short summary and verify the accordance with measurements on real traffic.

II. THE MODEL

Within the framework of this paper we only consider a one-dimensional ring of cells, each cell is 7.5 m long. The cells are either vacant or occupied by a vehicle labelled i . Its position is x_i and its discrete velocity is $v_i \in \{0, 1, \dots, v_{max}\}$. The gap g_i denotes the number of empty sites to its leading vehicle. The rules for a *parallel update* are

- Acceleration with regard to the vehicle ahead: $v_i \leftarrow \min(v_i + 1, g_i, v_{max})$,
- Noise: with a certain probability p_{dec} do: $v_i \leftarrow \max(v_i - 1, 0)$,
- Movement: $x_i \leftarrow x_i + v_i$.

One time step corresponds to 1 sec , hence $\Delta v = 1$ in the simulation corresponds to $\Delta v = 7.5\text{ m/s} = 27\text{ km/h}$ in reality. These rules describe a spatially and temporally discrete model. The investigated systems consist of L cells and N vehicles, the global density is $\rho = N/L$. The flow is defined as $J = \langle v \rangle \rho$ with the mean velocity $\langle v \rangle = \sum v_i / N$. In the following this standard model is denoted with SCA.

We extend our studies on further modifications of the SCA, the *slow-to-start* model (STS) [13,18] and the T^2 model designed by Takayasu and Takayasu [19]. The modifications are as follows: For the STS velocity-depending deceleration probabilities $p_{dec}(v_i)$ are employed with $p_{dec}(v_i = 0) = p_{dec} + p_{STS}$. Note that v_i is the velocity before the first update step is performed. In the T^2 model a further rule is added: standing vehicles with a headway $g_i = 1$ only accelerate with a certain acceleration probability $q_{acc} = 1 - p_{dec}(v_i = 0; g_i = 1)$ with $p_{dec}(v_i = 0; g_i = 1) = p_{dec} + p_{T^2}$. Unlike the SCA with similar parameters, both models exhibit a different behavior in the vicinity of the point of maximum flow ($\rho_{max} \equiv \rho(J_{max}), J_{max}$). They are capable to generate metastable states in the adiabatic approach, i.e. one finds two branches of $J(\rho)$ in a small interval around ρ_{max} . One of them is the stable one, the other is characterized by its finite life times, hysteresis loops can be found. Concluding we summarize:

$$\begin{aligned}
\text{SCA:} \quad & p_{dec} \neq p_{dec}(v_i), \\
\text{STS:} \quad & p_{dec}(v_i = 0) = \min(p_{dec} + p_{STS}, 1), \\
\text{T}^2: \quad & p_{dec}(v_i = 0; g_i = 1) = \min(p_{dec} + p_{T^2}, 1).
\end{aligned} \tag{1}$$

Actually, other definitions of $p_{dec}(v_i = 0)$ and $p_{dec}(v_i = 0; g_i = 1)$ are conceivable, but, for our purpose, we decided to use only the above ones.

III. SIMULATION RESULTS AND THEIR DISCUSSION

The density waves are moving upstream and can be easily observed in a space-time plot [7,20], one finds separation of dense and free-flow regions (Fig. 1). For the measurements it is necessary to introduce the mean local density of a cell k

$$\rho_k(t) \equiv \frac{1}{\lambda} \sum_{i=0}^{\lambda-1} \eta_{k+i} \quad \text{with} \quad \eta_{k+i} = \begin{cases} 1 & \text{if site } k+i \text{ is occupied} \\ 0 & \text{otherwise} \end{cases} \tag{2}$$

and an additional parameter λ that describes the length of the interval on which the local density has to be computed. It should satisfy the condition $\lambda_0 \ll \lambda \ll L$ [16] with a characteristic length scale λ_0 that is associated with the density fluctuations. On the other hand, one has to pay attention to the adjustment of the ratio λ/L in order to perform reliable simulations. For the determination of the jam velocity v_j we use the generalized T -point-auto-correlation function

$$C_{v_j}(r \equiv v_j^* \tau \Delta T, \tau) = \langle \prod_{\tau=0}^{T-1} \rho_k(x + v_j^* \tau \Delta T, t + \tau \Delta T) \rangle_L \tag{3}$$

with the supposed jam velocity $v_j^* \in [-1, 0]$. Among these v_j^* 's there is a value that develops $C_{v_j}(r, \tau)$ to the maximum. One has to scan the interval of all possible v_j^* 's until reaching the maximum of $C_{v_j}(r, \tau)$ – this is the desired real jam velocity v_j (Fig. 2). ΔT is the temporal distance between two single measurements which contributes to (3). Sufficiently large values of ΔT are necessary in order to observe a macroscopic motion and to determine v_j with an adequate accuracy. Unless otherwise mentioned, we set $L = 10^4$ and $\Delta T = 10^2$. This fix an accuracy $\Delta v_j = \pm 10^{-2}$ sites per time step. We are averaging over 20 measurements. The choice of parameters ensures that any finite size effects are excluded.

The inset of Fig. 2 points out that one has to adjust thoroughly the parameters T and ΔT . When T is of the order of magnitude of ΔT or larger the error of estimating v_j screens the accuracy of the measurement, C_{v_j} vanishes and the determination of all depending quantities fails. In other words, for $T/\Delta T > 1$ it plays an important rule that the jam velocity can be estimated with a higher accuracy. This problem becomes more serious while approaching ρ_c . In this region the calculations are complicated additionally because of the large fluctuations of C_{v_j} itself.

The jam velocity v_j depends on p_{dec} as it can be seen in Fig. 3 and is related to global quantities, see (7). We checked it for a variety of parameters, but could not notice any

remarkable deviations among the diverse sets of data. The modifications of the SCA, the STS and the T^2 , yield a different behavior, a small sample is also instanced in Fig. 3. The absolute values of the jam velocity in the models STS and T^2 are smaller than that of the SCA. This implies that both modifications are characterized by a lowered outflow from a jam that, in turn, reduces the jam velocity.

The results of simulations using the STS are basically shifted towards smaller $|v_j|$'s and proportional to p_{STS} , concurrent with increasing p_{STS} the function $v_j(p_{dec})$ becomes more and more linear (Fig. 3). Note that it is set $p_{STS} = \{0.3|0.5\}$ (1). p_{STS} can be recognized on the ordinate at $(p_{dec} = 0, |v_j| = p_{STS})$ and on the abscissa at $(p_{dec} = p_{STS}, |v_j| = 0)$. In the deterministic case ($p_{dec} = 0$) only the acceleration of standing vehicles is randomized. It is easy to see that the mean waiting time can be approached by a geometric series:

$$t_{det}^w = 0 \times q + 1 \times qp_{STS} + 2 \times qp_{STS}^2 + \dots = q \sum_{n=1}^{\infty} np_{STS}^n = \dots = \sum_{n=1}^{\infty} p_{STS}^n$$

with $p = 1 - p_{STS}$. That, in turn, directly leads to the jam velocity at $p_{dec} = 0$:

$$|v_j|_{det} = \frac{1}{t_{det}^w + 1} = 1 - p_{STS} \in [0, 1], \quad (4)$$

When p_{STS} exceeds $1 - p_{dec}$ a stopped vehicle will never be moved again and a complete deadlocks occurs.

The jam velocity of the T^2 model are also smaller than that of the SCA (Fig. 3). Here $p_{T^2} = \{0.5|1.0\}$ are applied (1). Starting from $p_{dec} = 1$ both the SCA and the T^2 yield similar measurements. This is valid as long as $p_{dec} \leq p_{T^2}$, since the noise of all vehicles screens other effects. But with decreasing p_{dec} the data differ. Now the reduced outflow from a jam results in slower movements of the density waves. If $p_{dec} = 0$ is reached the system is completely deterministic except the vehicles leading a jam. It takes not more than two time steps until this vehicle goes on. In this first time step its probability to accelerate is p_{T^2} . In the next time step its gap is larger than one and it can be advances without any restrictions, provided that is still standing. Hence the mean waiting time reads $t_{det}^w = p_{T^2} \in [0, 1]$ and yields

$$|v_j|_{det} = \frac{1}{t_{det}^w + 1} = \frac{1}{p_{T^2} + 1} \in [0.5, 1]. \quad (5)$$

Contrary to the STS, no deadlock situations arise for $p_{dec} < 1$.

Obviously, the measurements are strongly affected by the global vehicular density ρ . Below a critical density ρ_c the vehicles moves quite independent of each other, i.e. there is no correlation between them. For $\rho \geq \rho_c$ one finds upstream moving density waves which can be recognized in (3), e.g.

In the vicinity of the critical density ρ_c the jam velocity reveals large fluctuations (Fig. 4), otherwise it could be assumed to be constant. In the range where density waves are to be expected it is $v_j \neq v_j(\rho)$. This is originated in the independence between the outflow from

a jam and the global density. Nearby ρ_c the global and local flow cannot be characterized by equation (8), since many jams emerge and disappear again within a few time steps and the equilibrium ansatz fails. This causes the large fluctuations. We also find only a very weak dependence between v_j and v_{max} provided that v_{max} is sufficiently large (Fig. 5). For smaller quantities than depicted in Fig. 5 the measurements are strongly influenced by the relatively high probability of vehicles with $v = 0$, i.e. it is more likely that vehicles halt, but do not cause a stable jam.

Up to now we applied the auto-correlation function (3) to determine the jam velocity. But the quantity itself indicates the two different phases separated by a critical deceleration probability p_c (Fig. 6) or by a critical density ρ_c (Fig. 7). Varying p_{dec} leads to a transition while crossing p_c . Its clarity strongly depends on $T/\Delta T$, for insufficient ratios a plateau at $\bar{C}_{v_j}(p_{dec})$ occurs. Note, that the modified auto-correlation \bar{C}_{v_j} is defined as

$$\bar{C}_{v_j}(r, \tau) = \left\langle \left(\prod_{\tau=0}^{T-1} \rho_k(x + v_j^* \tau \Delta T, t + \tau \Delta T) \right)^{1/T} \right\rangle_L \quad (6)$$

and has the same dimension as the density, namely *veh/site*. The other transition takes place while crossing a critical density ρ_c . From a formal point of view it can be written as

$$C_{v_j}(\rho) = f(\rho) \Theta(\rho - \rho_c) \quad (7)$$

with the heavy side function Θ and a certain $f(\rho)$ that reflects the density dependence for $\rho > \rho_c$ (Fig. 7). For $\rho < \rho_c$ one finds empty regions of the order of magnitude of λ , and therefore C_{v_j} completely vanishes. Within the broadened transient range due to insufficient ratios λ/L a finite $C_{v_j}(\rho < \rho_c)$ renders only the possibility to find vehicles within λ and does not refer to a density wave. Thus, a small λ/L allows the estimation of ρ_c . On the other hand, for $\rho > \rho_c$ stable congestion emerge. The centroid of the same jam can be detected at $t_i = 0$ as well as at $t_f = \tau \Delta T > t_i$ located at $x(t_i) - |v_j|t_f$. Its higher density crucially contributes to C_{v_j} which remains finite during the whole simulation. For this purpose, ρ_c can be denoted as the density, at which long-term or never-ending jams emerge. It separates the densities according to (7). This transition is clarified in the inset of Fig. 7 with the modified auto-correlation $\bar{C}_{v_j}(\rho)$ (6). For a fixed density and a varying v_{max} the relationship can be estimated as $C_{v_j}(v_{max}) \propto \rho$ (Fig. 8).

How is the jam velocity related to other macroscopic quantities? In the steady state recognized by a conserved number and length of jams the dynamics are characterized by an equilibrium of out-flowing vehicles and vehicles attaching the jam from behind. The more frequent vehicles join the jam the faster the jam moves upstream. Since the free-flow region is located in the vicinity of the point of maximum flow (ρ_{max}, J_{max}) , the velocity of attaching vehicles is on average $\langle v_{att} \rangle = J_{max}/\rho_{max}$. The mean distance between the tail of the jam and the next vehicle is $\langle g \rangle = \rho_{max}^{-1} - 1$. Hence, we find the temporal distance

$$\Delta t_{att} = \frac{\langle g \rangle}{\langle v_{att} \rangle} \Leftrightarrow v_j = \frac{J_{max}}{\rho_{max} - 1} \leq 0. \quad (8)$$

This is confirmed by the simulation results depicted in Fig. 9. It means that v_j is essentially determined by the slope of the congested branch ($\rho \geq \rho_{max}$) in the fundamental

diagram. This can also be verified for the modifications SCA and T^2 (Fig. 10). The small deviations from the data drawn from simulations rest upon a difference between the outflow of the jam and the maximum global flow in the considered systems, but also in the above made assumption of the equilibrium. Actually, the lowered outflow from jams observed in the models SCA and T^2 in comparison to the SCA is also reflected by (8).

IV. SUMMARY

We investigated the cellular automaton model for vehicular traffic in order to get information about the density waves and the velocity of their centroids. Beside the standard cellular automata SCA we also included two of its modifications, the *slow-to-start* model SCA and the T^2 model. Both resemble the SCA except the rules for standing vehicles. Loosely spoken, they result in a lower flow downstream a jam. For the determination of the jam velocity and behavior of the model nearby the critical density ρ_c we used the auto-correlation function $C_{v_j}(r, \tau)$. Despite the high computational efforts ($\mathcal{O}(L^2)$) this method was suitable to be applied for our calculations.

The quantity $C_{v_j}(r, \tau)$ reflects the two different phases and depends on the global density ρ . The density regime is separated by the critical density ρ_c . For $\rho < \rho_c$ no stable jams emerge, whereas for larger ρ the system is dominated by sequences of dense and free-flow regions, where C_{v_j} remains finite and permits an estimation of ρ_c . At this point a jamming transition takes place. The transient region is smeared out. Both the local length λ and the number of calculations T have large effects on C_{v_j} .

Additionally, the correlation function includes information about the jam velocity. For sufficiently large ρ the absolute value of v_j is a continuous and descending function of p_{dec} , but it differs due to the chosen models. The differences between the models, especially for $p_{dec} \rightarrow 0$ and $p_{dec} \rightarrow 1$, could be explained phenomenologically by waiting time arguments. The jam velocity is essentially determined by the point (ρ_{max}, J_{max}) in the fundamental diagram, irrespective of the considered model.

Concluding, this knowledge enables a calibration of the SCA. Besides the approach of the fundamental diagram as known from records and data of real traffic a further point of interest is the velocity of upstream moving jams ($\approx -15 \text{ km/h}$ on German highways [21]) – but according to (8) all information is accumulated in the fundamental diagram, namely in the second characteristic slope of $J(\rho)$. Exemplary, for the SCA with vehicles of length one cell it is set $p_{dec} = 0.2 \cdots 0.3$ in order to calibrate the model for the simulation of traffic flow on German highways.

REFERENCES

- [1] D.E. Wolf, M. Schreckenberg and A. Bachem (eds.), *Traffic and Granular Flow* (World Scientific, Singapore, 1996).
- [2] M. Schreckenberg and D.E. Wolf (eds.), *Traffic and Granular Flow* (Springer, Singapore, 1998).
- [3] M.J. Lighthill and G.B. Whitham, in *Proc. Roy. Soc. of London A*, ed. by C. Herring (Cambridge, 1955), p. 281.
- [4] B.S. Kerner and P. Konhäuser, Phys. Rev. E **48** 4, 2335 (1993).
- [5] M. Bando, K. Hasebe, A. Nakayama, A. Shibata and Y. Sugiyama, Phys. Rev. E **51** 2, 1035 (1995).
- [6] D. Helbing, Phys. Rev. E **55** 3, 3735 (1997).
- [7] K. Nagel and M. Schreckenberg, J. de Phys. I **2**, 2221 (1992)
- [8] B. Chopard, P.O. Luthi and P.A. Queloz, J. of Phys. A **29**, 2325 (1996).
- [9] M. Rickert and K. Nagel, Int. J. of Mod. Phys. C **7** (1996).
- [10] J. Esser and M. Schreckenberg, J. Mod. Phys. (in press) (1997).
- [11] P. Wagner, K. Nagel and D.E. Wolf, Physica A **234**, 687 (1997).
- [12] A. Schadschneider and M. Schreckenberg, J. of Phys. A **26**, L697 (1992).
- [13] A. Schadschneider and M. Schreckenberg, J. of Phys. A **30**, L69 (1997).
- [14] A. Schadschneider and M. Schreckenberg, J. of Phys. A **31**, L225 (1998).
- [15] B. Eisenblätter, L. Santen, A. Schadschneider and M. Schreckenberg, Phys. Rev. E **57** 2, 1309 (1998).
- [16] S. Lübeck, M. Schreckenberg and K.D. Usadel, Phys. Rev. E **57** 1, 1171 (1998).
- [17] S. Krauß, P. Wagner and C. Gawron, Phys. Rev. E **55** 5, 5597 (1997).
- [18] R. Barlovic, L. Santen, A. Schadschneider, M. Schreckenberg, Euro. Phys. Journal B (in Press) (1998).
- [19] M. Takayasu and H. Takayasu, Fractals **1**, 860 (1993).
- [20] J. Treiterer, Ohio State University Technical Report No. PB 246094, Columbus Ohio (1975).
- [21] B.S. Kerner and H. Rehborn, Phys. Rev. E **53** 2, R1297 (1996).

FIGURES

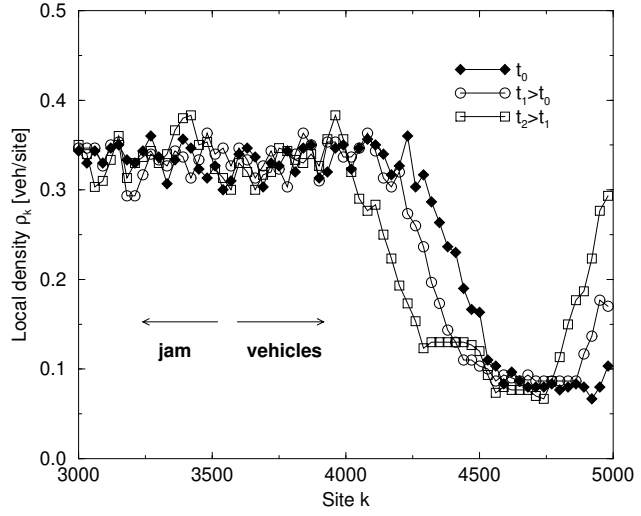


FIG. 1. Temporal evolution of the local density in the SCA – jam fronts and vehicles are moving in opposite directions. It is set $v_{max} = 5$, $p_{dec} = 0.5$ and $\lambda = 50$.

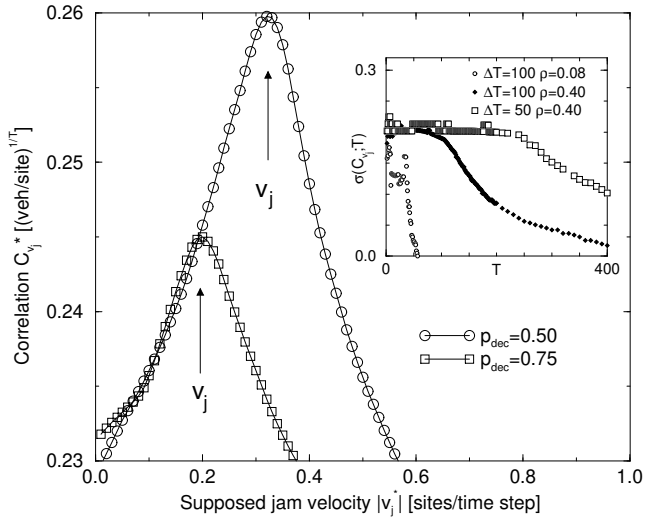


FIG. 2. The peak of the correlation function enables to estimate the jam velocity v_j ($v_{max} = 5$, $\lambda = 50$ and $\rho = 0.4$). The standard deviation of the symmetrically assumed C_{v_j} is depicted in the inset. For certain ratios $T/\Delta T$ the variance shrinks a lot. For an improper relationship the correlation function vanishes and inhibits the estimation of further quantities. In the vicinity of ρ_c this sensitivity is more pronounced and complicates the calculations. On the other hand, for shrinking ΔT the function C_{v_j} is significantly broadened and therefore its variance σ is higher.

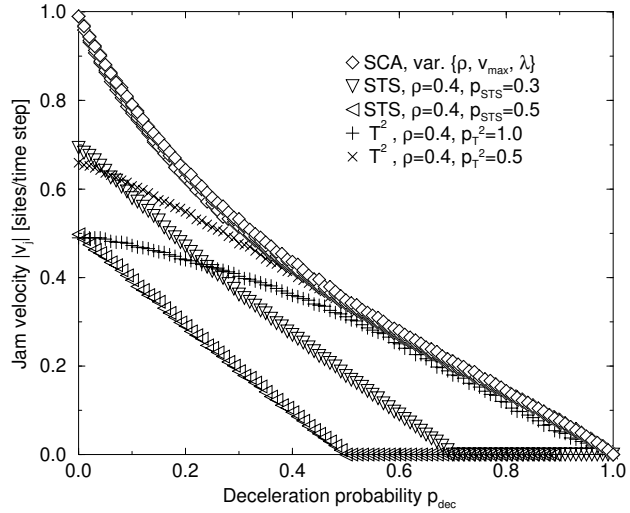


FIG. 3. The jam velocity as a function of p_{dec} depends on the considered model. The results of the SCA using various parameters and that of STS and T^2 differ obviously, the error bars are within the symbol size. Note that $v_{max} = 5$ and $\lambda = 30$ is set for STS and T^2 , whereas the choice of v_{max} does not influence the results for all models.

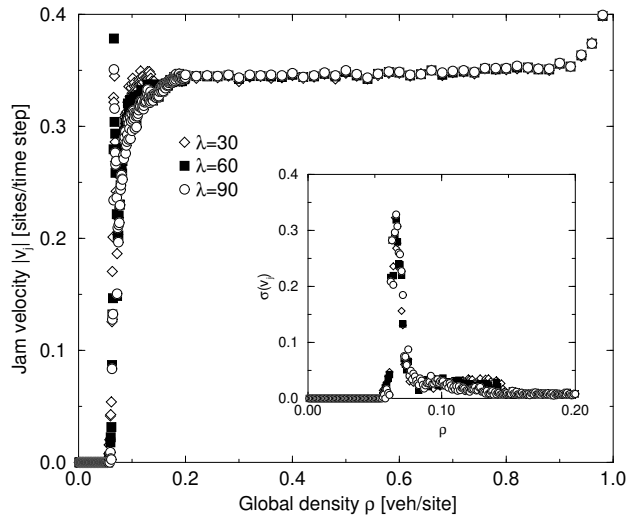


FIG. 4. Plot of $v_j(\rho)|_{v_{max}}$ for $v_{max} = 5$, $p_{dec} = 0.5$. Beyond ρ_c , especially for $0.2 \leq \rho \leq 0.8$, $v_j(\rho)$ can be assumed to be constant. The inset reveals the large fluctuations of v_j nearby ρ_c which are up to the order of magnitude of v_j itself.

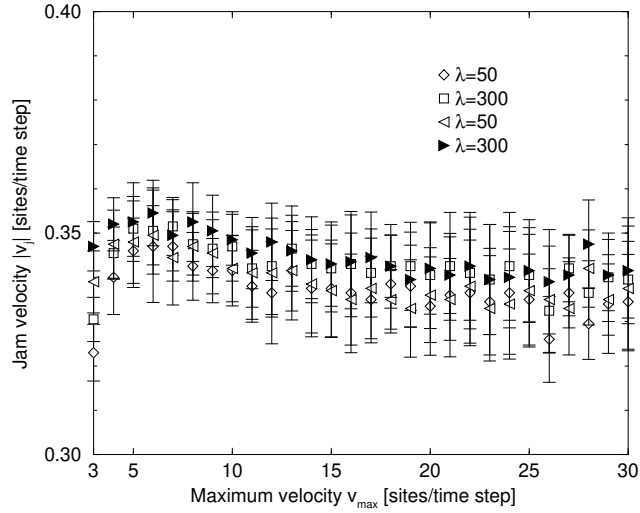


FIG. 5. Plot of $v_j(v_{max})$ for fixed ρ and $v_{max} = 5$, $p_{dec} = 0.5$. The data are located within the error bars quite well. They are weakly descending according to the fact that the maximum flow J_{max} depends on v_{max} .

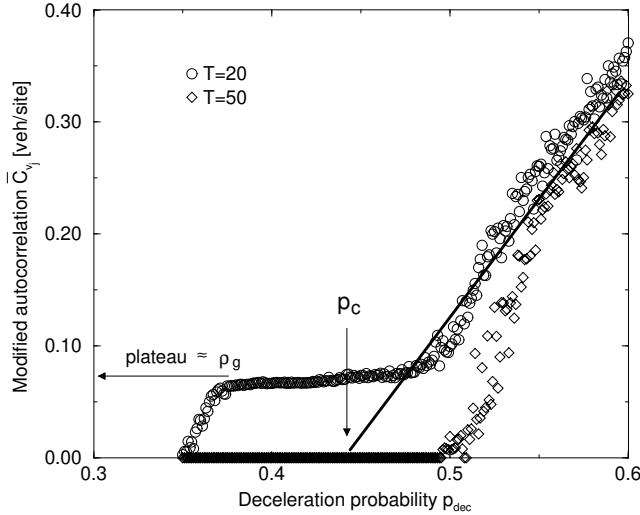


FIG. 6. The transition can also be obtained by varying the deceleration probability p_{dec} ($v_{max} = 5$). Here, the transition is smeared out due to finite size effects and systematic errors in the determination of \bar{C}_{v_j} (6). For small T a plateau at $\bar{C}_{v_j} = \rho_g$ can be identified near ρ_c . $\rho = 0.073$, $v_{max} = 5$ and $\lambda = 30$ are employed for both data sets, but T differs.

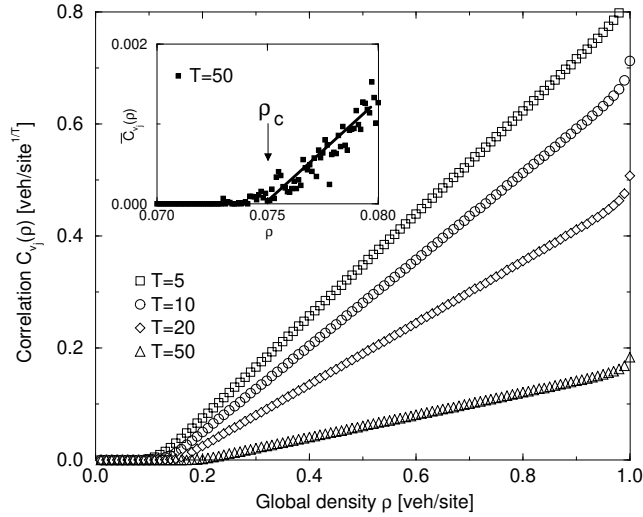


FIG. 7. Plot of the auto-correlation function $C_{v_j}(\rho)|_{v_{max}}$ for $v_{max} = 5$, $p_{dec} = 0.5$ and $\lambda = 30$. Below a signified density the correlation function vanishes due to the absence of stable jams. The inset zooms into the region $\rho \approx \rho_c$ for the modified auto-correlation $\bar{C}_{v_j}^{1/T}$ (6). As suggested by other results not published here that too large ratios λ/L broadens the transient region.

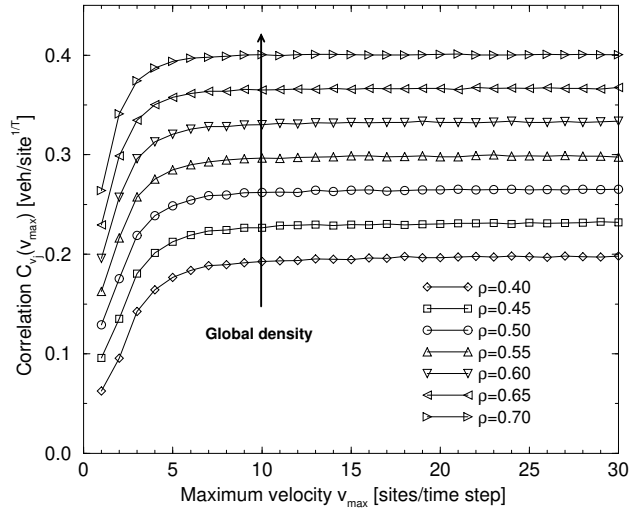


FIG. 8. Plot of the correlation function $C_{v_j}(v_{max})|_\rho$ for $p_{dec} = 0.5$ and $\lambda = 30$. A explanation similar to $v_j(v_{max})$ can be applied in order to discuss $C_{v_j}(v_{max})|_\rho$, but, in addition, there is a simple linear relationship between C_{v_j} and ρ .

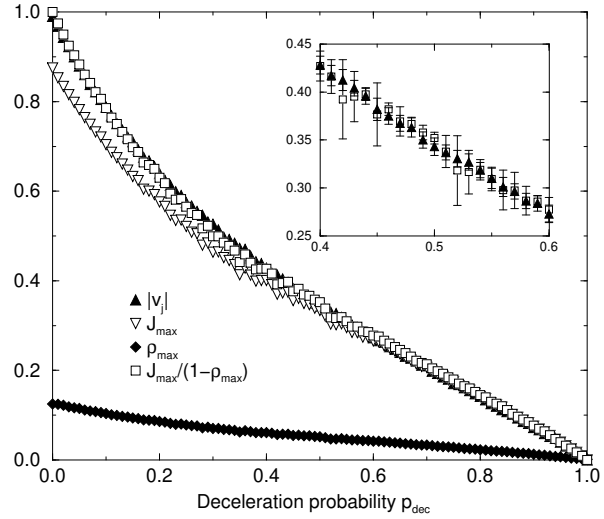


FIG. 9. The jam velocity can be explained by (8): $v_j = J_{max}/(\rho_{max} - 1)$ – a consequence of the phase separation for $\rho > \rho_c$. As shown in the inset, the data agree within the error bars, i.e. the jam velocity is directly related to the slope of the congested branch of a fundamental diagram ($v_{max} = 5$, $p_{dec} = 0.5$ and $\lambda = 30$).

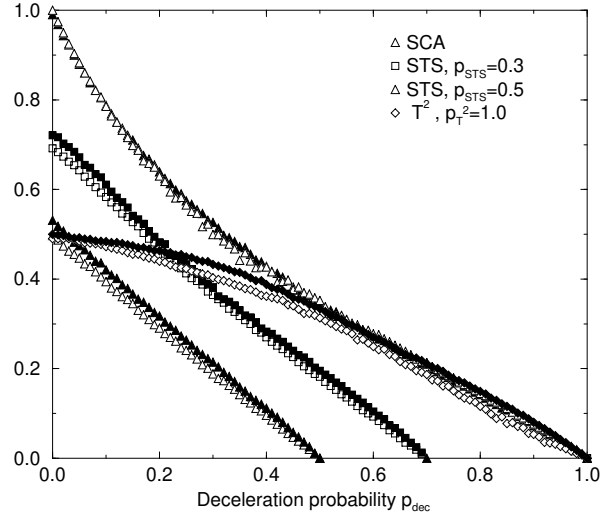


FIG. 10. v_j (filled symbols) for all used models ($v_{max} = 5$, $\lambda = 30$) are depicted as well as $J_{max}/(\rho_{max} - 1)$ (opaque symbols). The small deviations are related to the discrepancies between the outflow of a jam and the global maximum flow.